Effect of anisotropy on magneto-optical properties of uniaxial crystals: Application to CrO_2

Yu. A. Uspenskii
I. E. Tamm Theory Department, P. N. Lebedev Physical Institute, Russian Academy of Sciences, 117924 Leninskii Prospect 53, Moscow, Russia

E. T. Kulatov
General Physics Institute, Russian Academy of Sciences, 117942 Vavilov strasse 38, Moscow, Russia

S. V. Halilov
Max-Planck Arbeitsgruppe ''Elektronensysteme,'' Technische Universität, Abteilung Physik, D-01062 Dresden, Federal Republic of Germany
(Received 10 January 1996)

The effect of the magnetization direction **m** on the dielectric tensor of uniaxial crystals is described by a simple dependence of the gyration vector $\mathbf{g}(\omega)$ on **m**. It is shown that the vectors $\mathbf{g}(\omega)$ and **m** as well as the orbital magnetic moment $\langle\hat{\mathbf{L}}\rangle$ and **m** are generally aligned noncollinearly in contrast to an isotropic case. Formulas describing the polar Kerr effect are derived for crystals with their principal axis $c\perp\mathbf{m}$ and for polycrystals having *c* randomly oriented in the sample plane. Using these analytical results and performing *ab initio* calculations, we correctly reproduce anisotropy in optical spectra of CrO_2 and the main features in magneto-optical spectra of polycrystalline films of CrO_2. The maximal optical anisotropy and orientation dependence of $\mathbf{g}(\omega)$ of 100% are found in the energy interval $\hbar\omega\leqslant$ 2.1 eV coinciding with the direct half-metallic ferromagnetic gap of CrO_2. The noncollinearity effects in this interval are also very large. The obtained results correlate well with strong orientation dependence of $\langle\hat{\mathbf{L}}\rangle$ found in our calculations. [S0163-1829(96)07525-X]

I. INTRODUCTION

The large magnetic anisotropy of uniaxial crystals imposed by their symmetry makes them the favored materials for magneto-optical (MO) recording applications. A large variety of optical and MO measurements of uniaxial solids as well as measurements of their magnetic properties has been performed with a significant delay in their theoretical interpretation (see, e.g., Refs. 1,2 and references therein). The anisotropy in optical spectra of these materials has not been studied much, while systematic investigations of the orientation dependence of MO spectra are still in their beginning, although this phenomenon is closely related to the well-studied magnetic anisotropy. The phenomenon was experimentally investigated in detail only for hcp Co.[3,4] Subsequent *ab initio* calculations[5] excellently reproduced a significant difference in the values of the polar Kerr rotation for the magnetization orientations $\mathbf{M}\|[0001]$ and $\mathbf{M}\|[11\bar{2}0]$ which has been observed in Ref. 4. At the same time many questions concerning the MO anisotropy remain still open. Among others they are the structure of dielectric tensor of uniaxial crystals for the general direction of the magnetization, the expressions giving the polar Kerr rotation and the ellipticity for arbitrary orientation of the crystal, and the polar Kerr effect in polycrystalline materials consisting of uniaxial crystallites.

The present work considers the problems of MO anisotropy by both analytical and numerical methods. Detailed investigation is carried out for CrO_2. This compound, which is a widespread material for magnetic tape technology, crystallizes in the tetragonal (rutile) structure with $c/a=0.649\,58$ and orders ferromagnetically up to $T_C=391$ K.[6] Electronic structure calculations[7–9] characterize CrO_2 as a half-metallic ferromagnet (HMF) with metallic behavior for spin-majority electrons and a gap at the Fermi level for spin-minority electrons. Such a particular electronic structure can lead to the large MO effects as has been argued for PtMnSb.[10] Measurements show that the static conductivity of CrO_2 is nearly isotropic while the reflectivity spectra in the spectral interval $\hbar\omega=$ 0.5–2.0 eV are strongly anisotropic.[11] Observations of MO effects were somewhat contradictory. Early data[12] gave the extremum of ellipticity at 1.4 eV reaching 0.27°. Later investigations[13] showed no such extremum and found that the maximum of the Kerr rotation amounted to $|\theta_K|=0.15°$ at 3.7 eV. The orientation dependence of MO effects has not been studied yet, but judging by the significant anisotropy in optical spectra, one can expect the dependence to be rather strong.

The paper is organized as follows. Section II reviews briefly the microscopic theory of the dielectric tensor and analyzes its orientational dependence. We show that the anisotropy results in a noncollinear arrangement of the magnetization and the gyration vector and consider this outcome. Section III studies the polar Kerr effect in uniaxial crystals having the *c* axis parallel to the sample surface for normal light incidence. In this section we also find optical and MO characteristics of a polycrystalline sample: the reflectivity, the state of polarization of reflected light, the Kerr rotation, and the ellipticity. Section IV gives a brief description of our *ab initio* calculational method. Section V presents our calculated optical and MO spectra of CrO_2 and compares them with available experimental data. Much attention is given to

the orientation dependence of MO spectra. It is shown that in the spectral interval coinciding with the HMF gap width the gyration vector and the magnetization are strongly noncollinear and the reflected light has the maximum of noncoherence at these frequencies. Section VI summarizes the results and discusses the problems of interest.

II. FORM OF THE DIELECTRIC TENSOR IN UNIAXIAL FERROMAGNETIC CRYSTALS

Using general symmetry arguments, it is easy to show that the dielectric tensor of uniaxial crystals with the magnetization oriented along the c or a axis has the forms

$$\varepsilon^{[001]}=\begin{pmatrix} \varepsilon_{yy} & ig_{\parallel} & 0 \\ -ig_{\parallel} & \varepsilon_{yy} & 0 \\ 0 & 0 & \varepsilon_{zz} \end{pmatrix}, \tag{1}$$

$$\varepsilon^{[100]}=\begin{pmatrix} \varepsilon_{xx} & 0 & 0 \\ 0 & \varepsilon_{yy} & ig_{\perp} \\ 0 & -ig_{\perp} & \varepsilon_{zz} \end{pmatrix}. \tag{2}$$

Here and below the reference frame is defined by setting the z and x directions along the c and a crystal axes. For further consideration it is convenient to introduce the gyration vector $\mathbf{g}$ which is dual to the antisymmetric part of the tensor,[14]

$$\varepsilon^{a}_{\alpha\beta}=ie_{\alpha\beta\gamma}g_{\gamma}, \tag{3}$$

where $i=\sqrt{-1}$ and $e_{\alpha\beta\gamma}$ is the unit antisymmetric tensor. The antisymmetric part of Eqs. (1) and (2) is described by $\mathbf{g}\|\mathbf{m}$, as is directly guessed from the crystal symmetry [$\mathbf{m}=(\sin\vartheta\cos\varphi,\sin\vartheta\sin\varphi,\cos\vartheta)$ is a unit vector in the magnetization direction]. But for the general orientation of $\mathbf{m}$ group theory methods are not applicable and we must turn to the microscopic theory of the dielectric tensor.

The usually used random-phase-approximation-(RPA-) type expression for $\varepsilon_{\alpha\beta}$ has the form

$$\varepsilon_{\alpha\beta}(\omega)=\delta_{\alpha\beta}+\frac{4\pi^2e^2\hbar^2}{\Omega}\sum_{i,f}\int\frac{d\mathbf{k}}{E^2_{fi}(\mathbf{k})}j^{if}_{\alpha}(\mathbf{k})j^{fi}_{\beta}(\mathbf{k}) \times\frac{[\theta(E_f(\mathbf{k}))-\theta(E_i(\mathbf{k}))]}{\hbar\omega-E_{fi}(\mathbf{k})+i\delta}, \tag{4}$$

where i and f refer to the initial and final band states, $E_{fi}(\mathbf{k})=E_f(\mathbf{k})-E_i(\mathbf{k})$, Ω is the unit cell volume, and $j^{if}_{\alpha}(\mathbf{k})=\langle i\mathbf{k}|\hat{j}_{\alpha}|f\mathbf{k}\rangle$ is a matrix element (ME) of the current operator. In further analysis we will limit ourselves to the first order over spin-orbit interaction (SOI). Earlier a similar approach was successfully applied to the study of the orientation effect in cubic crystals.[15] In this approximation the antisymmetric part of tensor is written as[16]

$$\varepsilon^{a}_{\alpha\beta}(\omega)=\frac{4\pi^2e^2\hbar^2}{m^2\Omega}\sum_{i,f\neq i}\int\frac{d\mathbf{k}}{E^2_{fi}(\mathbf{k})}\left\{\frac{H^{i\prime}_{\mathrm{SO}}(\mathbf{k})}{E_{i\prime}(\mathbf{k})}[p^{\prime f}_{\alpha}(\mathbf{k})p^{fi}_{\beta}(\mathbf{k}) -(\alpha\leftrightarrow\beta)]+\frac{H^{f\prime}_{SO}(\mathbf{k})}{E_{f\prime}(\mathbf{k})}[p^{if}_{\alpha}(\mathbf{k})p^{\prime i}_{\beta}(\mathbf{k}) -(\alpha\leftrightarrow\beta)]\right\}\frac{[\theta(E_f(\mathbf{k}))-\theta(E_i(\mathbf{k}))]}{\hbar\omega-E_{fi}(\mathbf{k})+i\delta}, \tag{5}$$

where $p^{\prime f}_{\alpha}(\mathbf{k})$ is a ME of the momentum operator, band states are taken in the nonrelativistic approximation, and $H^{f\prime}_{\mathrm{SO}}(\mathbf{k})=\langle f\mathbf{k}|\xi(\mathbf{r})\hat{\boldsymbol{\sigma}}\hat{\mathbf{L}}|\prime\mathbf{k}\rangle$ is a ME of the SOI expressed in terms of

$$\xi(\mathbf{r})=\frac{\hbar}{4m^2c^2}\frac{1}{r}\frac{dV}{dr},$$

the spin operator $\hat{\boldsymbol{\sigma}}=\Sigma_{\alpha}\hat{\sigma}_{\alpha}\mathbf{e}_{\alpha}$, and the orbital moment operator $\hat{\mathbf{L}}$. To study a detailed structure of Eq. (5) we first consider the simplest case $\mathbf{m}=\mathbf{e}_z$ when nonrelativistic band states are pure spin up and spin down ones. For this case the diagonality of the momentum operator over spin indices results in the fact that only the part $\hat{\sigma}_z\hat{L}_z$ of the operator $\hat{\boldsymbol{\sigma}}\hat{\mathbf{L}}$ in the SOI gives a contribution to $\varepsilon^{a}_{\alpha\beta}(\omega)$. For the general magnetization direction $\mathbf{m}$ nonrelativistic band energies are unchangable by $\mathbf{m}$, while band eigenstates $|i\mathbf{k},\mathbf{m}\rangle$ can be written in the form $|i\mathbf{k},\mathbf{m}\rangle=\hat{U}(\mathbf{m})|i\mathbf{k},\ \mathbf{m}=\mathbf{e}_z\rangle$, where $\hat{U}(\mathbf{m})$ is the spin rotation matrix transforming spinors from the reference frame with the z direction along $\mathbf{m}$ to the frame with the z direction along the c axis. Owing to the unitarity of $\hat{U}(\mathbf{m})$, the ME's $p^{\prime i}_{\alpha}(\mathbf{k})$ do not depend on $\mathbf{m}$. Only the ME's $H^{i\prime}_{\mathrm{SO}}(\mathbf{k})$ show a dependence on $\mathbf{m}$ which can be reduced to the change from the operator $\hat{\sigma}$ to $\hat{\sigma}(\mathbf{m})=\hat{U}^{+}(\mathbf{m})\hat{\sigma}\hat{U}(\mathbf{m})=\mathbf{e}'_x\hat{\sigma}_x+\mathbf{e}'_y\hat{\sigma}_y+\mathbf{m}\hat{\sigma}_z$, where basic vectors $\mathbf{e}'_x$ and $\mathbf{e}'_y$ correspond to the reference frame with the z direction along $\mathbf{m}$. In doing so, we obtain for general direction of $\mathbf{m}$ nonzero ME's of the SOI having the form $H^{i\prime}_{\mathrm{SO}}(\mathbf{k})=\langle i\mathbf{k}|\xi(\mathbf{r})\hat{\sigma}_z\hat{\mathbf{L}}\mathbf{m}|\prime\mathbf{k}\rangle$. Here we took into account that band states $|i\mathbf{k}\rangle$ and $|\prime\mathbf{k}\rangle$ corresponding to $\mathbf{m}=\mathbf{e}_z$ have identical spin projections as follows from the diagonality of $p^{\prime f}_{\alpha}(\mathbf{k})$ and $p^{fi}_{\beta}(\mathbf{k})$ over spin indices. Using these considerations, Eq. (5) can be rewritten in the form showing a direct dependence of the gyration vector on $\mathbf{m}$:

$$\begin{aligned} g_{\alpha}(\omega)&=-ie_{\beta\gamma\alpha}\varepsilon^{a}_{\beta\gamma}(\omega)\\ &=-iG_{\alpha\beta}(\omega)m_{\beta}\\ &=-i\frac{4\pi^2e^2\hbar^2}{m^2\Omega}\sum_{i,f\neq i}\int\frac{d\mathbf{k}}{E^2_{fi}(\mathbf{k})}\\ &\quad\times\left\{\Pi_{\alpha}(\prime f,fi,\mathbf{k})\frac{H^{i\prime}_{\mathrm{SO},\beta}(\mathbf{k})}{E_{i\prime}(\mathbf{k})}\right.\\ &\quad\left.+\Pi_{\alpha}(if,\prime i,\mathbf{k})\frac{H^{f\prime}_{\mathrm{SO},\beta}(\mathbf{k})}{E_{f\prime}(\mathbf{k})}\right\}\frac{[\theta(E_f(\mathbf{k}))-\theta(E_i(\mathbf{k}))]}{\hbar\omega-E_{fi}(\mathbf{k})+i\delta}m_{\beta}, \end{aligned} \tag{6}$$

Here we introduced two axial vectors $\Pi_{\alpha}(\prime f,fi,\mathbf{k})=e_{\gamma\delta\alpha}[p^{\prime f}_{\gamma}(\mathbf{k})p^{fi}_{\delta}(\mathbf{k})-(\gamma\leftrightarrow\delta)]$ and $H^{i\prime}_{\mathrm{SO},\beta}(\mathbf{k})$

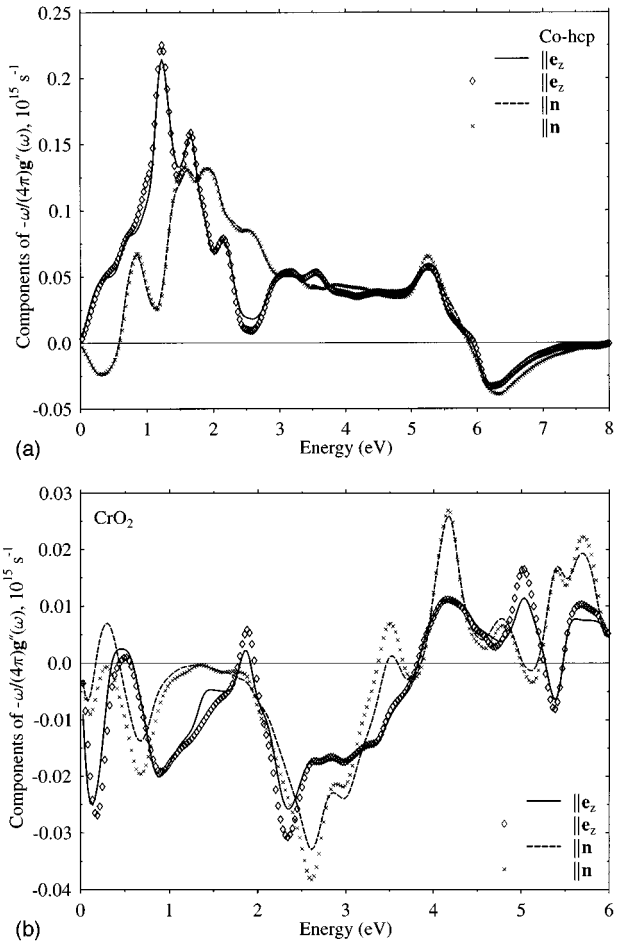

FIG. 1. Calculated components of $(-\omega/4\pi)\mathbf{g}''(\omega)$ for $\mathbf{m}=(1/\sqrt{2})(1,0,1)$ obtained from direct *ab initio* calculations and from Eq. (8): (a) results for hcp Co received from Eq. (8) are shown by the solid line (the component along $\mathbf{e}_z$) and the dashed line (the component along $\mathbf{n}$), rhombuses and crosses give respective results of direct calculations, (b) analogous results for CrO_2.

$=\langle i\mathbf{k}|\xi(\mathbf{r})\hat{\sigma}_z\hat{L}_\beta|\not{\mathbf{k}}\rangle$. It is important that the band energies and band states figuring in Eq. (6) be nonrelativistic, and so in the selection rules for the tensor $G_{\alpha\beta}(\omega)$ only the symmetry following from the crystal group should be taken into account. By these means the tensor $G_{\alpha\beta}(\omega)$ does not depend on $\mathbf{m}$ and must have the same form as the nonrelativistic dielectric tensor of uniaxial crystals:

$$G_{\alpha\beta}=\begin{pmatrix} G_{xx} & 0 & 0 \\ 0 & G_{xx} & 0 \\ 0 & 0 & G_{zz} \end{pmatrix}. \tag{7}$$

The associated form for the gyration vector is very simple and physically transparent:

$$\mathbf{g}(\omega)=\mathbf{e}_z\cos\vartheta\cdot g_\parallel(\omega)+\mathbf{m}_\perp\sin\vartheta\cdot g_\perp(\omega). \tag{8}$$

Here $\mathbf{m}_\perp=(\mathbf{e}_x m_x+\mathbf{e}_y m_y)/\sin\vartheta=(\cos\varphi,\sin\varphi,0)$ is the unit vector parallel to the projection of $\mathbf{m}$ on the ab plane and $g_\parallel(\omega)$, $g_\perp(\omega)$ are given by Eqs. (1),(2).

Equation (8) is the central result of this section. As its derivation was based on the approximate Equation (5), numerical testing of the accuracy of Eq. (8) is highly desirable. Figures 1(a) and 1(b) give our testing results for hcp Co and CrO_2 obtained in the case $\vartheta=\pi/4$ and $\varphi=0$. Because these calculations were carried out on rather sparse grids of $\mathbf{k}$ points, Figs. 1(a) and 1(b) show only upper estimates of the inaccuracy of Eq. (8) while its intrinsic inaccuracy is smaller, as discussed in Sec. IV. But even these results demonstrate small errors of Eq. (8) including frequency intervals with a 100% anisotropy of $\mathbf{g}(\omega)$ and the infrared region $\hbar\omega\leqslant\Delta E_{\mathrm{SO}}$, where Eq. (5) cannot be justified. Thus Eq. (8) can be considered as an accurate interpolating expression for $\mathbf{g}(\omega)$ even out of the application range of Eq. (5).

The vectors $\mathbf{g}(\omega)=\mathbf{g}'(\omega)+i\mathbf{g}''(\omega)$ and $\mathbf{m}$ are not collinear for the general magnetization direction, as seen from an alternative form of Eq. (8):

$$\mathbf{g}(\omega)=\mathbf{m}[g_\parallel(\omega)\cos^2\vartheta+g_\perp(\omega)\sin^2\vartheta] +\mathbf{n}[g_\parallel(\omega)-g_\perp(\omega)]\sin\vartheta\cos\vartheta, \tag{9}$$

where $\mathbf{n}=\mathbf{e}_z\sin\vartheta-\mathbf{m}_\perp\cos\vartheta$ is the unit vector orthogonal to $\mathbf{m}$. The real and the imaginary parts of $\mathbf{g}(\omega)$ are not collinear either:

$$\sin(\widehat{\mathbf{g}'\mathbf{g}''})=\sin 2\theta[g_\parallel'(\omega)g_\perp''(\omega)-g_\perp'(\omega)g_\parallel''(\omega)]/2|\mathbf{g}'||\mathbf{g}''|. \tag{10}$$

By these means a nonzero difference $g_\parallel(\omega)-g_\perp(\omega)$ leads to the noncollinearity of the three vectors $\mathbf{g}'(\omega)$, $\mathbf{g}''(\omega)$, and $\mathbf{m}$, which are collinear for isotropic media.

The above given argumentation can be successfully applied to the orientation dependence of the orbital moment $\langle\hat{\mathbf{L}}\rangle$. Using again the first order perturbation theory over the SOI and diagonality of the operator $\langle\hat{\mathbf{L}}\rangle$ over spin indices, it is easy to show that the dependence of $\langle\hat{\mathbf{L}}\rangle$ on $\mathbf{m}$ is given by equations analogous to Eq. (8) or (9), as can be directly guessed from the identical axial symmetry of $\langle\hat{\mathbf{L}}\rangle$ and $\mathbf{g}(\omega)$. Note that our orientation dependence of $\langle\hat{\mathbf{L}}\rangle\mathbf{m}$, given by an equation which is analogous to Eq. (9), is identical to the results obtained in Refs. 17–19. At the same time, our orbital moment has a component which is perpendicular to $\mathbf{m}$, and so $\langle\hat{\mathbf{L}}\rangle$ and $\mathbf{m}$ are not collinear. Returning to magneto-optics, we will try to correlate our results for $\mathbf{g}(\omega)$ with the orientation dependence of the polar Kerr rotation sketched in a broad outline for hcp metals.[4] Estimating $\theta_K(\omega)$ as proportional to $\mathbf{g}(\omega)\mathbf{m}$, we receive the orientation dependence of $\theta_K(\omega)$ which is perfectly analogous to that of $\langle\hat{\mathbf{L}}\rangle\mathbf{m}$. This similarity between orientation dependences of $\theta_K(\omega)$ and $\langle\hat{\mathbf{L}}\rangle\mathbf{m}$ was noted in Ref. 4. But the similarity becomes very approximate if we take into account the anisotropy in the diagonal components of the dielectric tensor and noncollinearity of $\mathbf{g}(\omega)$ and $\mathbf{m}$.

The noncollinearity of $\mathbf{g}'(\omega)$, $\mathbf{g}''(\omega)$, and $\mathbf{m}$ does not have any specific smallness, except material anisotropy. Our numerical results for the noncollinearity in CrO_2 will be discussed at the end of Sec. V. Here we only note that at some frequencies the values of $\mathbf{g}(\omega)\mathbf{n}$ are of 100% $\mathbf{g}(\omega)\mathbf{m}$ and the angle between $\mathbf{g}'(\omega)$ and $\mathbf{g}''(\omega)$ amounts up to $\pi/2$. The study of all the consequences of such a strong noncollinearity requires a special investigation. Here we mention the two most evident ones. First, there is no light propagation direc-

tion **s** meeting the condition $\mathbf{g}(\omega)\mathbf{s}=0$, and so the pure quadratic Cotton-Mouton effect is impossible. Second, in frequency intervals where $\mathbf{g}'(\omega)$ is nearly perpendicular to $\mathbf{g}''(\omega)$ the behavior of the observed gyration vector ranges from pure absorptive to pure dissipative, depending on **s**.

III. POLAR KERR EFFECT IN UNIAXIAL CRYSTALS FOR NORMAL INCIDENCE

The reflection of light incoming normal essentially depends on the material symmetry in the surface plane. Uniaxial crystals with the magnetization aligned perpendicularly to the surface (the polar configuration) and having the c axis oriented in the same direction are isotropic in the plane. Therefore expressions describing the polar Kerr effect in isotropic media are applied for them. The situation becomes much more complicated if a crystal has the c axis oriented in the surface plane. For this case, by setting the z direction normal to the surface, the x direction along the c axis, and the y direction along the a axis, we obtain the dielectric tensor in the following form:

$$\varepsilon_{\alpha\beta}=\begin{pmatrix} \varepsilon_{xx} & \varepsilon_{xy} & 0 \\ -\varepsilon_{xy} & \varepsilon_{yy} & 0 \\ 0 & 0 & \varepsilon_{zz} \end{pmatrix}. \tag{11}$$

As follows from Eq. (11), two light beams propagating along the z direction have complex refractive indices n given by the equation

$$n_{\pm}^2=\overline{\varepsilon}\pm\sqrt{\delta\varepsilon^2-\varepsilon_{xy}^2}, \tag{12}$$

where $\overline{\varepsilon}=(\varepsilon_{xx}+\varepsilon_{yy})/2$ and $\delta\varepsilon=(\varepsilon_{xx}-\varepsilon_{yy})/2$. The key quantity of light reflection is the amplitude reflection matrix $r_{\alpha\beta}^{(0)}$ connecting incident and reflected electric fields: $E_{\alpha}^{(r)}=r_{\alpha\beta}^{(0)}E_{\beta}^{(i)}$. Here and later, the indices α, β refer only to the x, y directions, because for normal light incidence the xy plane alone is important. Using the continuity of transverse components for electric and magnetic fields and carrying out some transformations, we find

$$r_{xx}^{(0)}\equiv\overline{\varrho}+\delta\varrho=\overline{\varrho}+\overline{\varrho}_{\varepsilon}\delta\varepsilon\frac{\mathrm{Det}+2\varepsilon_{xy}^2}{\mathrm{Det}},$$

$$r_{yy}^{(0)}\equiv\overline{\varrho}-\delta\varrho=\overline{\varrho}-\overline{\varrho}_{\varepsilon}\delta\varepsilon\frac{\mathrm{Det}+2\varepsilon_{xy}^2}{\mathrm{Det}},$$

$$r_{xy}^{(0)}=-r_{yx}^{(0)}=\overline{\varrho}_{\varepsilon}\varepsilon_{xy}, \tag{13}$$

where $\mathrm{Det}=\varepsilon_{xx}\varepsilon_{yy}+\varepsilon_{xy}^2$ and $\varrho_{\pm}\equiv(1-n_{\pm})/(1+n_{\pm})=\varrho\pm\overline{\varrho}_{\varepsilon}\sqrt{\delta\varepsilon^2-\varepsilon_{xy}^2}$.

Until this moment the Cartesian basic vectors were related to the c and a crystal axes. Now the x direction is related to the direction of the electric field in the incident light wave. A new amplitude reflection matrix is

$$r_{\alpha\beta}=U_{\alpha\gamma}(\phi)r_{\gamma\delta}^{(0)}U_{\delta\beta}(-\phi)=\begin{pmatrix} \overline{\varrho}+\delta\varrho\cos2\phi & \delta\varrho\sin2\phi+\overline{\varrho}_{\varepsilon}\varepsilon_{xy} \\ \delta\varrho\sin2\phi-\overline{\varrho}_{\varepsilon}\varepsilon_{xy} & \overline{\varrho}-\delta\varrho\cos2\phi \end{pmatrix}, \tag{14}$$

where $U(\phi)$ is the rotation matrix, with ϕ being an angle between the old and new x directions. The reflected light wave is elliptically polarized, with the ellipse orientation given by an angle ψ and the major axes ratio b/a. It is convenient to express these quantities in terms of the Stokes parameters[20]

$$\psi=\tfrac{1}{2}\arctan(S_2/S_1),$$

$$b/a=\tan\left[\frac{1}{2}\arcsin\left(\frac{S_3}{\sqrt{S_1{}^2+S_2{}^2+S_3{}^2}}\right)\right], \tag{15}$$

where S_i are the Stokes parameters,

$$S_0=|E_x^{(r)}|^2+|E_y^{(r)}|^2=(|r_{xx}|^2+|r_{yx}|^2)|\mathbf{E}^{(i)}|^2,$$

$$S_1=|E_x^{(r)}|^2-|E_y^{(r)}|^2=(|r_{xx}|^2-|r_{yx}|^2)|\mathbf{E}^{(i)}|^2,$$

$$S_2=E_x^{(r)}E_y^{(r)*}+E_x^{(r)*}E_y^{(r)}=(r_{xx}r_{yx}^*+r_{xx}^*r_{yx})|\mathbf{E}^{(i)}|^2,$$

$$S_3=\frac{1}{i}(E_x^{(r)}E_y^{(r)*}-E_x^{(r)*}E_y^{(r)})=\frac{1}{i}(r_{xx}r_{yx}^*-r_{xx}^*r_{yx})|\mathbf{E}^{(i)}|^2. \tag{16}$$

It is seen that ψ and b/a arise from off-diagonal components of $r_{\alpha\beta}$ and have origins in nonzero values of $\delta\varrho\sin2\phi$ and $\overline{\varrho}_{\varepsilon}\varepsilon_{xy}$. The MO contributions to rotation and ellipticity can be distinguished as odd over ε_{xy}, corresponding to the usual measurement procedure which includes the reverse of magnetization. Denoting $\psi=\psi^{(0)}+\theta_K$ and $b/a=(b/a)^{(0)}+\epsilon_K$, where θ_K and ϵ_K are MO rotation and MO ellipticity, we have

$$\psi^{(0)}=\tfrac{1}{2}\arctan(\mathrm{Re}\tau),$$

$$(b/a)^{(0)}=\tan[\tfrac{1}{2}\arcsin(\mathrm{Im}\tau)],$$

$$\tau=\frac{\sin2\phi(\varrho_x-\varrho_y)}{\varrho_x\cos^2\phi+\varrho_y\sin^2\phi},$$

$$\theta_K+i\epsilon_K=-\frac{2\varepsilon_{xy}(\varrho_x-\varrho_y)}{(\varepsilon_{xx}-\varepsilon_{yy})(\varrho_x\cos^2\phi+\varrho_y\sin^2\phi)}. \tag{17}$$

In the derivation of these equations we neglected terms which are quadratic in $\delta\varrho\sin2\phi$ or $\overline{\varrho}_{\varepsilon}\varepsilon_{xy}$ and used the notation: $\varrho_x=(1-\sqrt{\varepsilon_{xx}})/(1+\sqrt{\varepsilon_{xx}})$ and $\varrho_y=(1-\sqrt{\varepsilon_{yy}})/(1+\sqrt{\varepsilon_{yy}})$ with ε_{xx} and ε_{yy} given by Eq. (11). In the two simplest cases when $\mathbf{E}^{(i)}\|c$ or $\mathbf{E}^{(i)}\perp c$ ($\phi=0$ or $\pi/2$), rotation and ellipticity are exclusively of MO origin. Neglecting in Eq. (17) the terms which are quadratic in $\sqrt{\varepsilon_{xx}}-\sqrt{\varepsilon_{yy}}$, we can reproduce the result obtained for these particular cases in Ref.21.

Considering the polar Kerr effect in polycrystalline materials which have the c axis randomly oriented in the sample plane, we suppose that a crystallite size is somewhat larger than the penetration length of light but is much smaller than the light beam diameter, as is typical for many polycrystals. The total intensity of reflected light is a sum of a great number of intensities reflected from individual crystallites. Therefore, to find the macroscopic quantities θ_K and ϵ_K we must use Eqs. (15) with the Stokes parameters averaged over

ϕ. It may be shown that this approach perfectly agrees with the usual procedure for measurement of θ_K by rotating a linear polarizer to the total intensity minimum and measurement of ϵ_K by a $\lambda/4$ phase shifter and applying the Senarmont principle.[2] Using this approach, we have for polycrystals

$$\theta_K + i\epsilon_K = -\overline{\varrho_\varepsilon}\varepsilon_{xy}/\overline{\varrho} = \frac{2\varepsilon_{xy}}{(\sqrt{\varepsilon_{xx}}+\sqrt{\varepsilon_{yy}})(1-\sqrt{\varepsilon_{xx}\varepsilon_{yy}})} \tag{18}$$

and $\psi^{(0)} = (b/a)^{(0)} = 0$. We emphasize that the polar Kerr rotation and ellipticity for polycrystals are not the values obtained from the standard isotropic expressions with $\overline{\varepsilon} = (\varepsilon_{xx}+\varepsilon_{yy})/2$. If the optical anisotropy is 100%, the difference between Eq. (18) and such approximate calculations can be very significant. The inverse procedure of finding ε_{xy} from experimental θ_K and ϵ_K obtained with a polycrystalline sample can also be incorrect in the case of a large anisotropy of crystallites. A similar situation has taken place in $La_{2-x}Sr_xCuO_4$ where first optical measurements carried out on polycrystalline samples showed a prominent maximum of optical conductivity at 0.5 eV. But subsequent experiments on single crystals[22] as well as theoretical investigations[23] proved that this maximum is an artifact of isotropic equations applied to a polycrystal.

Our approach based on averaged Stokes parameters can also be used to find the reflectivity of polycrystalline materials and the state of polarization of reflected light:

$$R(\omega) = \langle S_0\rangle/|\mathbf{E}^{(i)}|^2 = |\overline{\varrho}|^2 + |\delta\varrho|^2 + |\varrho_\varepsilon\varepsilon_{xy}|^2,$$

$$P(\omega) = \sqrt{\langle S_1\rangle^2+\langle S_2\rangle^2+\langle S_3\rangle^2}/\langle S_0\rangle = 1 - \frac{|\delta\varrho|^2}{|\overline{\varrho}|^2+|\delta\varrho|^2+|\overline{\varrho_\varepsilon}\varepsilon_{xy}|^2}. \tag{19}$$

The reflected light is not perfectly coherent since crystallites are randomly oriented. This fact results in a nonzero value of $1-P(\omega)$ which indicates the microscopic optical anisotropy of material while other optical parameters characterize a polycrystal as isotropic media.

IV. CALCULATION METHOD

Our self-consistent electronic structure calculations of CrO_2 were carried out by the linear muffin-tin orbital (LMTO) method[24] with the local spin density approximation (LSDA) exchange-correlation potentials[25] and atomic sphere radii equal to $2.130a_B$, $2.130a_B$, $1.618a_B$, and $1.618a_B$ for Cr, O, and the first and second empty sites, respectively. Our atomic sphere charges and spin moments practically coincided with those of Ref. 9; the band structure and density of states closely agreed with the results of earlier investigations.[7–9] The thus obtained crystal potentials were used then in relativistic band structure calculations which included the SOI in the Hamiltonian but used the nonrelativistic basic set.

The absorptive part of dielectric tensor was calculated from Eq. (4) and smoothed with $\Gamma = 0.1$ eV while the dissipative part was found from the Kramers-Kronig transformation in the energy interval $\hbar\omega \leqslant 21.8$ eV. The intraband Drude contribution was taken with the parameters $\hbar\omega_p = 1.4$ eV and $\gamma_D = 0.11$ eV, which are within the limits given in the experimental work.[11] The polar Kerr rotation and ellipticity of crystals of CrO_2 with $\mathbf{m}=(0,0,1)$ and $\mathbf{m}=(1,0,0)$ were obtained from Eq. (17) and of polycrystals of CrO_2 from Eq. (18). The relativistic band structure calculations for these two magnetization directions were carried out with a grid of 512 **k** points in the 1/8 part of the Brillouin zone (BZ). More details of our calculation method for the dielectric tensor can be found in Refs. 26–28.

In order to test the orientation dependence of the gyration vector given by Eq. (8), we carried out additional calculations of the dielectric tensor for hcp Co and CrO_2. Testing this equation, it is important to calculate its left- and right-hand sides with equal accuracy. For this reason, the same grid of **k** points in the 1/2 part of the BZ was used for the orientations $\mathbf{m}=(0,0,1)$, $(1,0,0)$, and $(1/\sqrt{2})(1,0,1)$. Since relativistic band structure calculations in the 1/2 part of BZ are very time consuming, we carried them out on rather sparse grids and found that Eq. (8) is satisfied better as a number of **k** points increases. Figures 1(a) and 1(b) show our most accurate results for hcp Co and CrO_2 obtained with 1960 **k** points over 1/2 the BZ and with 822 **k** points, respectively. These results give us upper estimates of the inaccuracy of Eq. (8). But the intrinsic inaccuracy of Eq. (8) is smaller, judging from the fact that several times as many **k** points must be used to reproduce all details of $\mathbf{g}(\omega)$ in the visible spectral region and about 50 000 **k** points are required for this aim in the infrared spectral region.[27]

V. ANISOTROPY MANIFESTATIONS IN OPTICAL AND MAGNETO-OPTICAL SPECTRA OF CrO_2

In this section we present our *ab initio* results for the dielectric tensor, optical properties, the polar Kerr effect, and the orbital moment of CrO_2, considering anisotropy effects at full length. We start with a discussion of the dielectric tensor components calculated for the magnetization directions $\mathbf{m}\|c$ and $\mathbf{m}\perp c$. Figure 2 shows the real and the imaginary parts of the diagonal components $\varepsilon_{xx}(\omega)$ and $\varepsilon_{zz}(\omega)$ compared with experimental data.[11] Here and below the Cartesian basic vectors $\mathbf{e}_x$ and $\mathbf{e}_z$ are oriented along the *a* and *c* axes. Because both calculations with $\mathbf{m}\|c$ and with $\mathbf{m}\perp c$ give very close results for the diagonal components of the tensor, only dependences for $\mathbf{m}\perp c$ are presented here. By and large, calculations correctly reproduce the behavior of $\varepsilon_{xx}(\omega)$ and $\varepsilon_{zz}(\omega)$ with pronounced features at $\hbar\omega = 0.7$ eV, 1.9 eV, and 2.9 eV. The difference between $\varepsilon_{xx}(\omega)$ and $\varepsilon_{zz}(\omega)$ is also reproduced well; namely, $\varepsilon_{zz}(\omega)$ has a much stronger feature at 0.7 eV while $\varepsilon_{xx}(\omega)$ has a more prominent one at 1.9 eV. Disagreements between theory and experiment are limited to a downward shift of calculated dependences $\varepsilon_1(\omega)$ for $\hbar\omega \leqslant 1$ eV and too low values of $\varepsilon_2(\omega)$, especially $\varepsilon_{2,zz}(\omega)$, near 1.5 eV. It should be noted that our optical conductivity $\sigma_{1,xx}(\omega) = \omega\varepsilon_{2,xx}(\omega)/(4\pi)$ excellently agrees with the calculation of Ref. 29 . The latter also shows too small a value of $\sigma_{1,xx}(\omega)$ at $\hbar\omega = 1.5$ eV.

Figure 3 presents our spin decomposition of the optical conductivity $\sigma_{1,xx}(\omega)$. A 2.1-eV-wide gap observed for spin-minority electrons is the result of the half-metallic ferromagnetic state of CrO_2. Its smearing arises from the SOI hybrid-

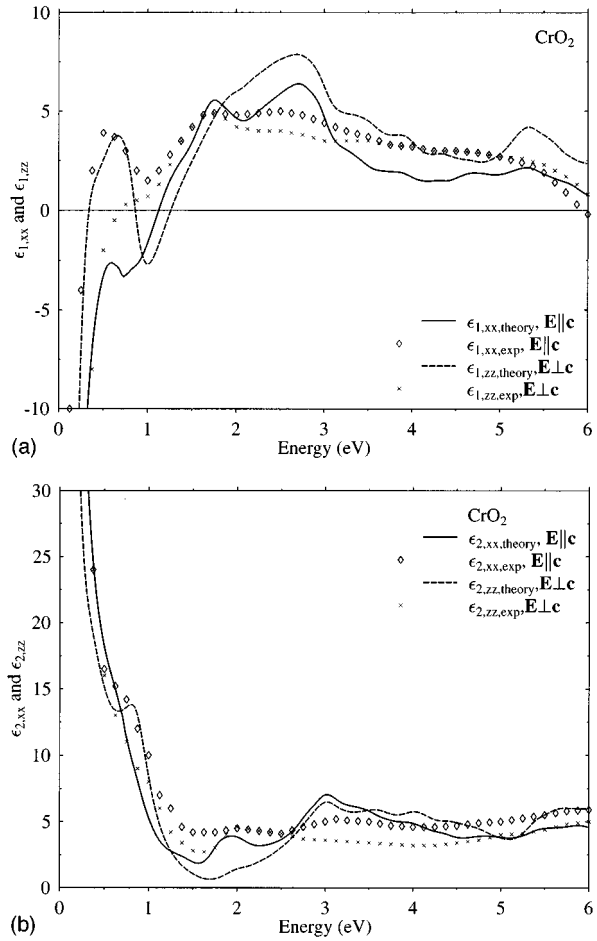

FIG. 2. Calculated and experimental diagonal components of the dielectric tensor of CrO_2: (a) the real part, (b) the imaginary part. The dependences are shown as follows: calculations with $\mathbf{E}\|c$ (solid line) and with $\mathbf{E}\perp c$ (dashed line), experimental data of Ref. 11 with $\mathbf{E}\|c$ (rhombs), and with $\mathbf{E}\perp c$ (crosses).

ization of spin-majority and spin-minority electronic states. This decomposition shows that the features at 0.7 eV and 1.9 eV are caused by spin-majority electronic excitations while the feature at 2.9 eV is in fact the HMF gap feature arising from excitations of spin-minority electrons.

Off-diagonal components of the dielectric tensor $\varepsilon_{xy}(\omega)$ and $\varepsilon_{yz}(\omega)$ were calculated with the magnetization directions $\mathbf{m}\|\mathbf{e}_z$ and $\mathbf{m}\|\mathbf{e}_x$, respectively. Broadly speaking, both values $\sigma_{2,xy}(\omega)=-\omega\varepsilon_{1,xy}(\omega)/(4\pi)$ and $\sigma_{2,yz}(\omega)=-\omega\varepsilon_{1,yz}(\omega)/(4\pi)$ have rather similar behavior with pronounced extrema at 0.2 eV, 0.6 eV, 2.8 eV (double feature), 4.1 eV, and 5.7 eV (Fig. 4). But this similarity does not advance beyond common outlines. Careful consideration reveals significant differences in the amplitudes, shapes, and, partly, positions of these features. The strongest orientation dependence is observed in the energy interval $\hbar\omega=1$–2 eV, at 4.1 eV and at 5.7 eV. Notice that for $\hbar\omega=1$–2 eV values of $\varepsilon_{2,zz}(\omega)$ and $\varepsilon_{1,yz}(\omega)$ are significantly smaller than the respective values $\varepsilon_{2,xx}(\omega)$ and $\varepsilon_{1,xy}(\omega)$, which indicates small matrix elements $p_z^{if}(\mathbf{k})$ in this energy interval. Additional information on the spectra of $\sigma_{yz}(\omega)$ is gained from their spin decomposition (Fig. 5). It is seen that features at 0.2 eV and 0.6 eV falling withing the HMF gap are due to

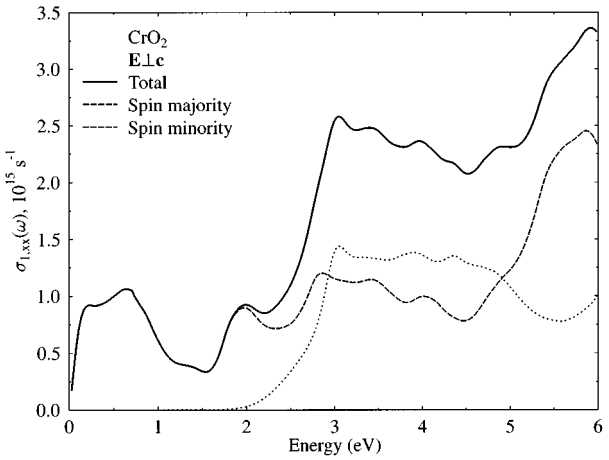

FIG. 3. Spin decomposition of the interband diagonal optical conductivity $\sigma_{1,xx}(\omega)$ of CrO_2 with $\mathbf{E}\perp c$. The total dependence is shown by the solid line, spin-majority contribution by the dashed line, and spin-minority contribution by the dotted line.

spin-majority excitations. For energies above the gap both spin contributions have approximately equal amplitudes and identical signs. Only nearby $\hbar\omega=5.1$ eV do spin contributions have opposite signs and strongly cancel each other.

The polar Kerr rotation and ellipticity are influenced by both the orientation dependence of off-diagonal components and the anisotropy of diagonal components of the dielectric tensor. Figure 6 shows the polar Kerr rotation $\theta_K(\omega)$ calculated for two magnetization orientations: $\mathbf{m}\|c$ and $\mathbf{m}\perp c$ with the light polarizations $\mathbf{E}\|a$ and $\mathbf{E}\|c$ for the latter. One can see that the orientaion effect is very significant for CrO_2 especially at $\hbar\omega=0.7$–2.1 eV. The effect of the light polarization, i.e., of anisotropy in the diagonal components, is not so large. In Fig. 7 we compare our results for a polycrystalline sample of CrO_2 which were obtained from Eq. (18) with experimental data of Ref. 13 received for CrO_2 films with the c axis randomly oriented in the film plane. The calculation reproduced whole dependences of $\theta_K(\omega)$, $\epsilon_K(\omega)$ and positions of the main features rather well while values of $|\theta_K|$

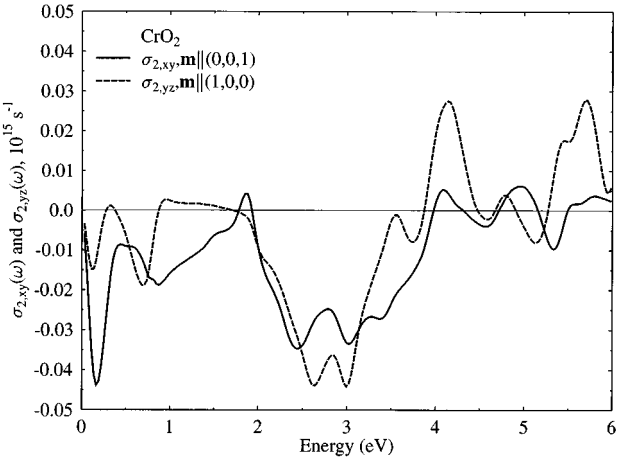

FIG. 4. Imaginary part of the off-diagonal conductivity CrO_2 calculated for $\mathbf{m}=(0,0,1)$ and $\mathbf{m}=(1,0,0)$. The dependence $\sigma_{2,xy}(\omega)$ is shown by the solid line and $\sigma_{2,yz}(\omega)$ by the dashed line.

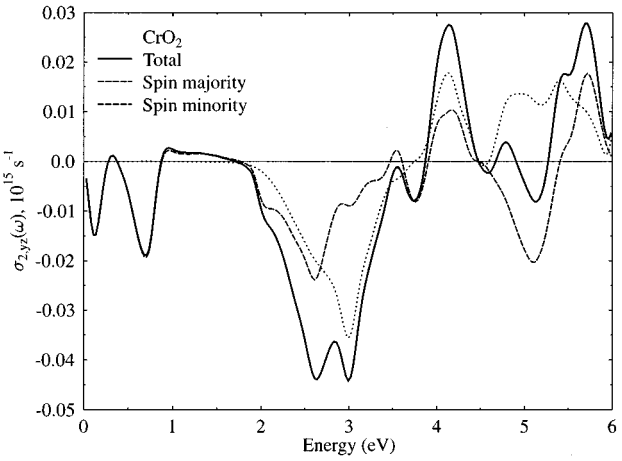

FIG. 5. Spin decomposition of $\sigma_{2,yz}(\omega)$ of CrO_2. The total dependence is shown by the solid line, spin-majority contribution by the dashed line, and spin-minority contribution by the dotted line.

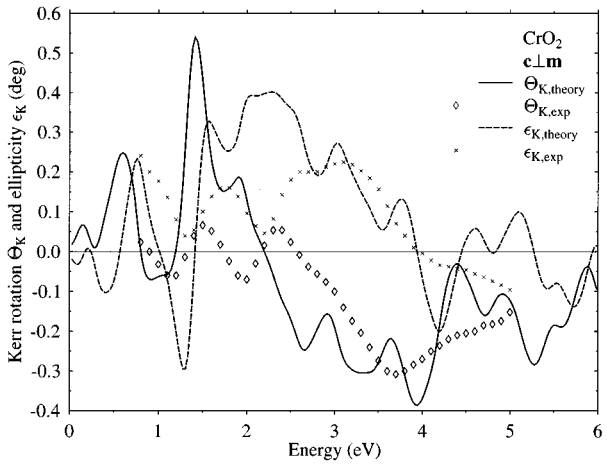

FIG. 7. Calculated and experimental results for the polar Kerr rotation and ellipticity of polycrystalline films of CrO_2 with $c\perp\mathbf{m}$. The dependences are shown as follows: calculated $\theta_K(\omega)$ (solid line), calculated $\epsilon_K(\omega)$ (dashed line), and experimental data of Ref. 13 for $\theta_K(\omega)$ (rhombs) and for $\epsilon_K(\omega)$ (crosses) (for convenience of comparison the experimental data are given as multiplied by the factor of 2).

and $|\epsilon_K|$ are twice as large as experimental ones on average. The largest disagreement is observed at 1.4–2.5 eV where the calculated maximum of $\theta_K(\omega)$ at 1.5 eV has a very large amplitude, and the maximum at 1.9 eV is shifted by 0.35 eV downward in energy and is separated from the first one by the minimum being too weak in comparison with the experiment.[13] One can easily find that too large values of $\theta_K(\omega)$ and $\epsilon_K(\omega)$ at $\hbar\omega=1.5$ eV arise mainly from too low values of the calculated diagonal components at this energy. Really, the calculation gives $|\varepsilon_{zz}(\omega)|=2.7$ at $\hbar\omega=1.5$ eV against the experimental value $|\varepsilon_{zz}(\omega)|=5.9$.[11] This difference leads to a strong enhancement of the calculated $\theta_K(\omega)$ and $\epsilon_K(\omega)$ because the quantity $\theta_K(\omega)+i\epsilon_K(\omega)$ is proportional to the factor $|\varepsilon_{\rm diag}|^{-1/2}|\varepsilon_{\rm diag}-1|^{-1}\approx|\varepsilon_{\rm diag}|^{-3/2}$ which is approximately 3.2 times larger than the experimental one. On the other hand, a too weak splitting of the maxima calculated at 1.5 eV and 1.9 eV could serve as an indication of the importance of non-muffin-tin effects which might be significant for CrO_2 possessing the open rutile structure and which were ignored in our calculations. Another possible reason is the high sensitivity of $\theta_K(\omega)$ and $\epsilon_K(\omega)$ to the crystal orientation at $\hbar\omega=0.7$–2.3 eV which is clearly demonstrated by Fig. 6. Owing to this sensitivity, any film texture or material microstructure details which were not taken into account in our model of a polycrystal can result in significant changes of $\theta_K(\omega)$ and $\epsilon_K(\omega)$ at these frequencies. It seems possible that the significant difference between the experimental data of Refs. 12,13 is just connected with this fact.

Concluding this section we discuss several characteristic manifestations of anisotropy in CrO_2 compound predicted from our calculations. The first one is the frequency dependence of the state of polarization $P(\omega)$ for the light reflected from a polycrystal with the c axis randomly oriented in the sample plane. This value calculated from Eq. (19) is a signal of crystallite anisotropy going from a macroscopically isotropic polycrystalline sample. Figure 8 shows that the minimum of $P(\omega)$ is obtained in the same frequency interval where optical constants are most anisotropic. Note that the absolute value of $1-P(\omega)$ is not large but sufficient for receiving experimental information about optical anisotropy by this way. The second manifestation is connected with the

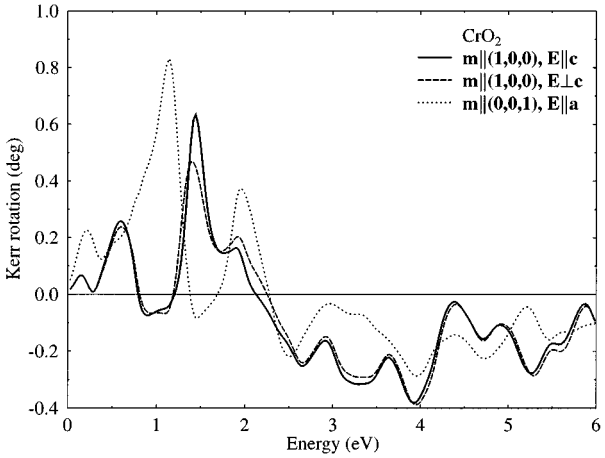

FIG. 6. Calculated results for the polar Kerr rotation of $CrO_2$with $\mathbf{m}=(1,0,0)$ and $\mathbf{E}\|\mathbf{c}$ (solid line), with $\mathbf{m}=(1,0,0)$ and $\mathbf{E}\perp c$ (dashed line), and with $\mathbf{m}=(0,0,1)$ (dotted line).

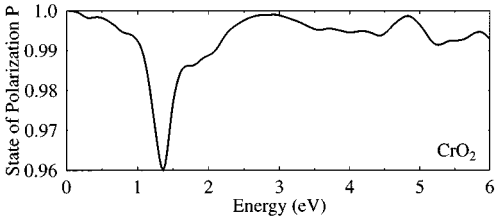

FIG. 8. Calculated frequency dependence of the state of polarization $P(\omega)$ for light reflected from a polycrystalline film of CrO_2.

noncollinearity of the magnetization and the gyration vector for the general orientation of **m**. Figure 9 gives components of the gyration vector, which are parallel and perpendicular to **m**, in the case of $\mathbf{m}=(1/\sqrt{2})(1,0,1)$. One can see that the component parallel to **m** dominates in sum, but in the energy interval $\hbar\omega=$ 1–2 eV amplitudes of parallel and perpendicular components are approximately equal. In addition, in this energy interval the real and the imaginary parts of the gyration vector are strongly noncollinear and even close to orthogonality (Fig. 10). By this means, in this spectral interval noncollinearity effects are so significant that modification of the standard scheme used for MO calculations in isotropic and cubic solids seems to be necessary. The third manifestation is noncollinearity of the orbital and spin moments for the general orientation of **m**. Our calculations give $\langle\hat{\mathbf{L}}\rangle=-0.053$ and -0.01 μ_B/cell for $\mathbf{m}=(0,0,1)$ and $(1,0,0)$. Such a large orientation effect for $\langle\hat{\mathbf{L}}\rangle$ leads to an angle of 34° between $\langle\hat{\mathbf{L}}\rangle$ and $-\mathbf{m}$ for $\vartheta=45°$.

VI. SUMMARY AND DISCUSSION

Using first-order perturbation theory, we studied the orientation dependence of the gyration vector and found that for the general direction of the magnetization, the vectors $\mathbf{g}(\omega)$ and **m** are not collinear and the real and the imaginary parts of the gyration vector are also not collinear. Numerical testing carried out for hcp Co and CrO_2 showed the high accuracy of the orientation dependence of $\mathbf{g}(\omega)$ following from Eq. (8). For normal light incidence we derived expressions describing the polar Kerr effect in uniaxial crystals and in polycrystals consisting of uniaxial crystallites [Eqs. (17),(18)]. These expressions shall be used in the case of 100% optical anisotropy when simplified approaches of an effective isotropic type are not justified by any means.

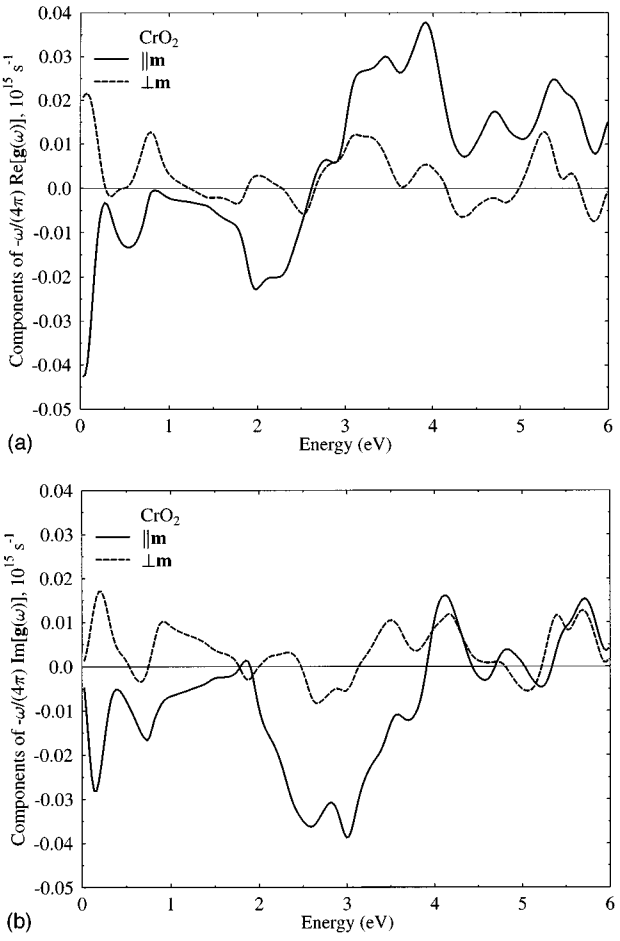

FIG. 9. Calculated components of the gyration vector of CrO_2 for $\mathbf{m}=(1/\sqrt{2})(1,0,1)$: (a) the real part (b) the imaginary part. The component of $[(-\omega)/4\pi]\mathbf{g}(\omega)$ which is parallel to **m** is shown by the solid line and perpendicular to **m** by the dashed line.

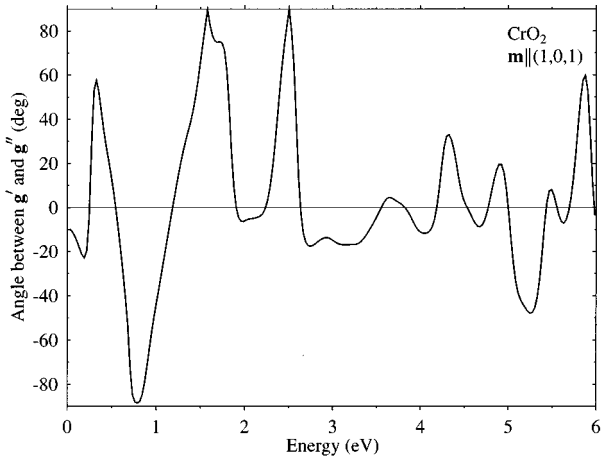

FIG. 10. Calculated frequency dependence of the angle between $\mathbf{g}'(\omega)$ and $\mathbf{g}''(\omega)$ of CrO_2 for $\mathbf{m}=(1/\sqrt{2})(1,0,1)$.

Our *ab initio* calculations of CrO_2 correctly described the anisotropy in optical spectra of this compound and predicted a large orientation dependence of the MO spectra in the energy interval $\hbar\omega=$ 0.7–2.3 eV. Using Eq. (18), we also calculated the MO spectra of polycrystalline films. The calculated dependences successfully reproduced the main features of the experimental spectra but had amplitudes larger by a factor of 2. We emphasize that the energy interval $\hbar\omega\leqslant$ 2.1 eV which approximately coincides with the direct HMF gap of CrO_2 is characterized by the maxima of both optical anisotropy and orientation dependence. In this interval the light reflected from the polycrystalline sample has a significant noncoherence, $\mathbf{g}(\omega)$ strongly deviates from **m**, and the angle between $\mathbf{g}'(\omega)$ and $\mathbf{g}''(\omega)$ is rather large, amounts to $\pi/2$. The listed factors are qualitatively new in comparison with the isotropic case. They significantly complicate the description of MO phenomena in uniaxial crystals for the general magnetization direction, and so an appropriate modification of the theory is necessary. At the same time, the MO spectra of uniaxial crystals in the intervals of maximal orientation dependence seem to be more sensitive to sample preparation and to the details of the measurement procedure.

ACKNOWLEDGMENTS

This work was partially supported by the Russian Fund of Basic Investigations Grant No. 94-02-03680-a. One of us (Y.A.U.) is grateful to Professor J. Kübler for helpful discussions on the electronic structure of CrO_2. He acknowledges the Sonderforschungsbereich 252-Darmstadt/Frankfurt/Mainz for financial support during the visit.

[1] K.H.J. Buschow, in *Handbook on Ferromagnetic Materials*, edited by E.P. Wohlfarth and K.H.J. Buschow (North-Holland, Amsterdam, 1988), Vol. 4, p. 493; W. Reim and J. Schoenes, *ibid.*, Vol. 5, p. 133.
[2] J. Schoenes, in *Materials Science and Technology*, edited by R.W. Cahn, P. Haasen, and E.J. Kramer (Verlag-Chemie, Weinheim, 1992), Vol. 3, p. 147.
[3] E.A. Ganshina, G.S. Krinchik, L.S. Mironova, and A.S. Tablin, Zh. Éksp. Teor. Fiz. **78**, 733 (1980) [Sov. Phys. JETP **51**, 369 (1980)].
[4] D. Weller, G.R. Harp, R.F.C. Farrow, A. Cebollada, and J. Sticht, Phys. Rev. Lett. **72**, 2097 (1994).
[5] G.Y. Guo and H. Ebert, Phys. Rev. B **50**, 10 377 (1994).
[6] B.L. Chamberland, Cri. Rev. Solid State Sci. **7**, 1 (1977).
[7] K. Schwarz, J. Phys. F **16**, L211 (1986).
[8] E.T. Kulatov and I.I. Mazin, J. Phys. Condens. Matter. **2**, 343 (1990).
[9] S. Matar, G. Demazeau, J. Sticht, V. Eyert, and J. Kübler, J. Phys. (Paris) **2**, 315 (1992).
[10] R.A. de Groot, F.M. Mueller, P.G. van Engen, and K.H.J. Buschow, Phys. Rev. Lett. **50**, 2024 (1983).
[11] L.L. Chase, Phys. Rev. B **10**, 2226 (1974).
[12] A.M. Stoffel, J. Appl. Phys. **40**, 1238 (1969).
[13] H. Brändle, D. Weller, S.S.P. Parkin, J.C. Scott, P. Fumagalli, W. Reim, R.J. Gambino, R. Ruf, and G. Güntherodt, Phys. Rev. B **46**, 13 889 (1992).
[14] L.D. Landau and E.M. Lifshitz, *Electrodynamics of Condensed Media* (Pergamon, New York, 1960).
[15] S.V. Halilov, J. Phys. Condens. Matter **4**, 1299 (1992).
[16] P.N. Argyres, Phys. Rev. **97**, 334 (1955).
[17] H. Brooks, Phys. Rev. **58**, 909 (1940).
[18] G.S. Fletcher, Proc. Phys. Soc. London A **67**, 505 (1954).
[19] P. Bruno, Phys. Rev. B **39**, 865 (1989).
[20] M. Born and E. Wolf, *Principles of Optics* (Pergamon, New York 1964).
[21] P. Fumagalli, Ph.D. thesis, ETH-Zürich, 1990 (cited in Ref. 2).
[22] S. Tajima *et al.*, Mod. Phys. Lett. B **1**, 383 (1988).
[23] I.I. Mazin, E.G. Maksimov, S.N. Rashkeev, S.Yu. Savrasov, and Yu.A. Uspenskii, Pis'ma Zh. Éksp. Teor. Fiz. **47**, 94 (1988) [JETP Lett. **47**, 113 (1988)].
[24] O.K. Andersen, Phys. Rev. B **12**, 3060 (1975).
[25] U. von Barth and L. Hedin, J. Phys. C **5**, 1629 (1972).
[26] Yu.A. Uspenskii, E.G. Maksimov, S.N. Rashkeev, and I.I. Mazin, Z. Phys. B **53**, 263 (1983).
[27] Yu.A. Uspenskii and S.V. Halilov, Zh. Éksp. Teor. Fiz. **95**, 1022 (1989) [Sov. Phys. JETP **68**, 588 (1989)].
[28] Yu.A. Uspenskii, E.T. Kulatov, and S.V. Halilov, Zh. Éksp. Teor. Fiz. **107**, 1708 (1995) [Sov. Phys. JETP **80**, 952 (1995)].
[29] H. Brändle, D. Weller, J.C. Scott, J. Sticht, P.M. Oppeneer, and G. Güntherodt, in *Proceedings of the International Conference on the Physics of Transition Metals*, Darmstadt, Germany, 1992, edited by P.M. Oppeneer and J. Kübler (World Scientific, Singapore, 1993), Vol. 1, p. 345.